1-dimensional modelling and simulation of the calcium looping process

Jaakko Ylätalo[a,*], Jouni Ritvanen[a], Borja Arias[b], Tero Tynjälä[a], Timo Hyppänen[a]

[a] *Lappeenranta University of Technology, LUT Energy, P.O. Box 20, Finland*
[b] *Instituto Nacional del Carbon, CSIC-INCAR Spanish Research Council, Oviedo, Spain*

Abstract

Calcium looping is an emerging technology for post-combustion carbon dioxide capture and storage in development. In this study, a 1-dimensional dynamical model for the calcium looping process was developed. The model was tested against a laboratory scale 30 kW test rig at INCAR-CSIC, Spain. The study concentrated on steady-state simulations of the carbonator reactor. Capture efficiency and reactor temperature profile were compared against experimental data. First results showed good agreement between the experimental observations and simulations.

Keywords: calcium looping process, process modelling, CCS, dual circulating fluidised beds

1. Introduction

Limiting anthropogenic emissions that accelerate the climate change has been a hot topic during the past decade. There are numerous methods and scenarios to limit those emissions from industry, agriculture, transportation, and other sources. With the growing demand of energy and abundance of some fossil fuels, interest has grown towards methods limiting stationary anthropogenic emissions from, for example, power plants burning coal. One promising method could be calcium looping process. Post-combustion calcium looping process was first introduced by Shimizu et al. [1]. The process utilizes the reversible reaction between calcium oxide and carbon dioxide.

$$\mathrm{CaO} + \mathrm{CO_2} \rightleftharpoons \mathrm{CaCO_3} \tag{1}$$

Stationary CO_2 flows to a fluidised bed reactor, carbonator, where CO_2 reacts with calcium oxide producing calcium carbonate. Carbonation reaction is exothermic and the thermal energy produced can be utilized to improve the efficiency of the process the efficiency of the process alongside with other high temperature flows of the process. Calcium carbonate is transferred to a another fluidised bed reactor, calciner, where it is regenerated back to calcium oxide producing a high concentration CO_2 flow. The high concetration CO_2 flow can be compressed and stored. Calcination reaction is endothermic and requires thermal energy. This thermal energy can be provided by burning a fraction of the combustor fuel with oxygen. Also thermal coupling with the boiler has been proposed [2]. A schematic of the process is presented in Figure 1.

The high flow rates of CO_2 produced by power plants require sufficient residence times and a good gas-solid contact to achieve reasonable reactor sizes and economical feasibility [3]. This is best achieved in fluidised bed reactors. A variety of fluidised bed combinations can be used in the calcium looping process but this study concentrates on two interconnected circulating fluidised beds [4]. Computational models can be valuable tools in the development of systems and processes. They often save time and money by removing the need to build a full-scale pilot plant. Computational models also pose challenges in describing the process accurately, because they always contain assumptions and simplifications to some degree. By finding the fundamental phenomena and parameters governing the process, a reliable model can be created.

*Corresponding author
Email address: jaakko.ylatalo@lut.fi (Jaakko Ylätalo)

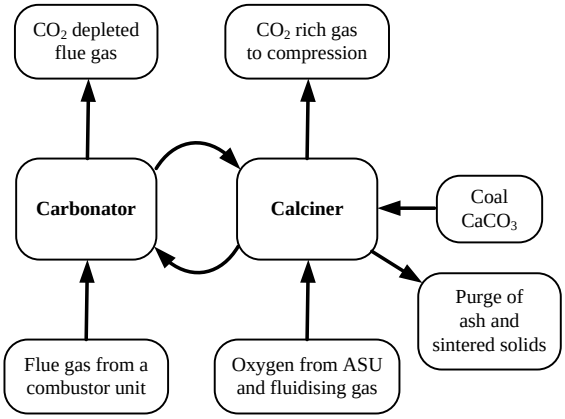

Figure 1: Calcium looping process

Many studies have been done recently regarding the characteristics of this process. Earlier studies [3, 5, 6, 7, 8] related to modelling of calcium looping process have concentrated purely on stationary cases. In some cases [3, 6] only one of the reactors is modelled. In contrast to earlier models, the model presented in this paper is capable of solving unsteady situations and solves 1 dimensional (1-D) conservation equations for mass, energy and conversion degree for both interconnected fluidised bed reactors of the calcium looping process. Thus, the model is capable to consider the effects of chemical reactions, heat and mass transfer in each vertical reactor level based on calculated local values of temperatures, gas and solid concentrations. In previous studies, the energy balance and incomplete mixing have not been considered which limits the capability of process models to model detailed process phenomena in a physical and accurate manner. Each reactor is discretized using the control volume method into vertical 1-D control volumes. The mass and energy balances are solved at each time step using a build-in solver within Matlab/Simulink. Phenomena like solid entrainment, heat transfer, and chemical reactions are modelled with semi-empirical correlations. In the following chapters, the modelling principles will be introduced and steady-state results from a laboratory-scale experimental setup will be compared against the model results. The comparison will concentrate on the carbonator reactor and steady-state results; more experimental data is needed to make further analysis. The 1-D carbonator model reactivity, hydrodynamics, and energy balance have been validated as a result of this comparison.

2. Theory of calcium looping process

Calcium looping process is based on the fast reaction between calcium oxide and CO_2. However, the fast reaction period is limited by the formation of a $CaCO_3$ product layer to the interior and exterior of the particle. After the formation of the product layer the reaction is controlled by slow diffusion which is unsuitable for CO_2 capture purposes. [9, 10]

Describing this decay of the carrying capacity is essential to the accuracy of the model. Natural limestone undergoing carbonation-calcination cycles quickly reaches an asymptotical conversion degree limit. Mass based conversion degree for the material is defined as

$$W = \frac{m_{\mathrm{CaCO3}}}{m_{\mathrm{CaO}} + m_{\mathrm{CaCO3}}} \tag{2}$$

where m_{CaCO3} is the mass of calcium carbonate and m_{CaO} is the mass of calcium oxide. In a mix of different aged limestones the conversion degree limit is defined as the averaged maximum conversion degree [9]. Carbonation reaction rate is modelled with a correlation presented by Shimizu et al. [1]

$$r_{\mathrm{carb}} = m_{\mathrm{s}} \left(W_{\mathrm{max}} - W\right) k_{\mathrm{carb}} \left(C_{\mathrm{CO2}} - C_{\mathrm{CO2e}}\right) \tag{3}$$

where m_s is the total solid mass, $(W_{max} - W)$ represents the active fraction of solid material and k_{carb} is the kinetic constant for the carbonation reaction. The optimal temperature of carbonation has been determined to be around 650 °C when treating flue gases at atmospheric pressure [3]. When the temperature rises, reaction kinetics improve, but also the equiblibrium CO_2 partial pressure increases causing the reaction to slow down or change direction. When considering the operation temperature, the carbonator has a narrow operation window, which has to be taken into account in the modelling. Efforts to improve sorbent durability againts the decay of activity and attrition are ongoing, but natural limestones can provide the required activity if it is possible to use sufficient make-up flows of limestone.

Unlike the carbonation reaction, the calcination reaction is mainly controlled by the surrounding temperature and the CO_2 partial pressure. The temperature of the calciner is recommeded to be below 950 °C because of operational factors and the increasing decay of activity above 1000 °C [9, 10]. A reaction rate correlation for the calcination reaction was presented by Garcia-Labiano et al. [11]. Calcination reaction rate depends on the properties of the limestone and the relation of CO_2 partial pressure p_{CO2} to the equilibrium partial pressure p_{CO2}.

$$r_{calc} = m_s W S_{ave} \frac{M_{CaCO3}}{\rho_{CaCO3}} k_{calc} \left(1 - \frac{p_{CO2}}{p_{CO2e}}\right) \tag{4}$$

where S_{ave} is the reaction surface area, M_{CaCO3} is the molar mass of calcium carbonate, ρ_{CaCO3} is the material density of calcium carbonate, and k_{calc} is the kinetic parameter for the calcination reaction of the selected limestone.

3. Description of modelling approach

The studied calcium looping process consists of two fast gas fluidised risers and solids return systems after the risers. Each reactor is discretized using the control volume method into vertical 1-D control volumes. Spatial derivatives are discretized using first-order approximations with central difference or upwind scheme for convective fluxes. Time dependent balance equations for mass and energy are written for each element. A set of time dependent equations is solved using fixed-step explicit ordinary differential equation solver in Simulink/Matlab system. Steady state solutions are obtained by a dynamic simulation until steady state is obtained. Each element is treated as an ideally mixed control volume. Solid and gas phases are calculated separately using the same average temperature for both of the phases. Modules can be either adiabatic or prescribed insulation thickness and surface temperature can be determined. There is also an option for additional internal heat exchangers.

3.1. Gas phase

The gas phase consists of four gas components, namely O_2, N_2, CO_2 and H_2O. For each gas component j at element i, the mass fraction w is solved using the general time dependent mass balance

$$\frac{dw_{i,j}}{dt} = \frac{1}{m_{g,i}} \left(\dot{m}_{i,j,in} - \dot{m}_{i,j,out} + r_{i,j}\right) \tag{5}$$

where $m_{g,i}$ is the total gas mixture mass at element i and $r_{i,j}$ is the source term of the gas component j from chemical reactions. The total gas mixture mass is solved using the ideal gas approach

$$m_{g,i} = \frac{p V_{g,i} M_{g,i}}{R T_i} \tag{6}$$

where the gas mixture volume is $V_{g,i} = V_{tot,i} - V_{s,i}$ and the molar mass of the gas mixture

$$M_{g,i} = \left(\sum_j \frac{w_{i,j}}{M_j}\right)^{-1} \tag{7}$$

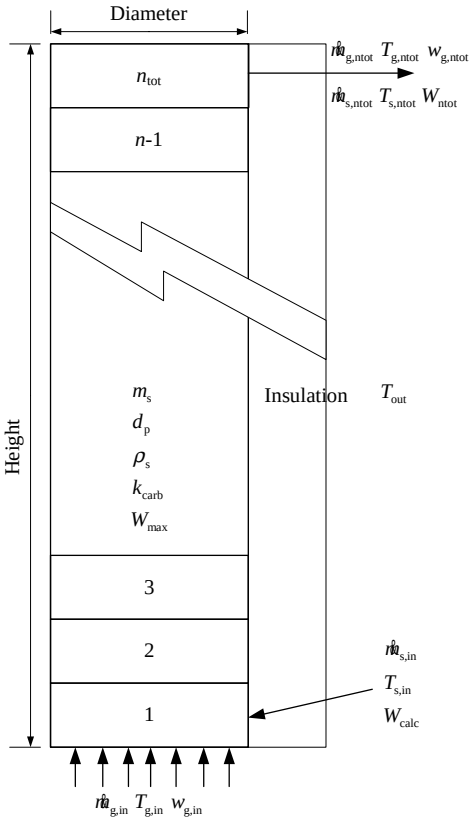

Figure 2: Calculation parameters and boundary conditions for the simulation. The outlet boundary condition equals the values solved in the last control volume n_{tot}, for example the exit temperature of phases is the same as the temperature in the last element

In the carbonator, the reaction rate is defined for the formation of $CaCO_3$ and the reaction reduces the amount of CO_2. Thus, the source term of CO_2 for the carbonator is then

$$r_{\mathrm{CO_2},i} = -r_{\mathrm{carb},i}\frac{M_{\mathrm{CO_2}}}{M_{\mathrm{CaO}}}. \tag{8}$$

In the calciner, the reaction rate is defined for the formation of CaO and the reaction increases the amount of CO_2. Thus, the source term of CO_2 for the calcinator is then

$$r_{\mathrm{CO_2},i} = r_{\mathrm{calc},i}\frac{M_{\mathrm{CO_2}}}{M_{\mathrm{CaCO3}}}. \tag{9}$$

Heterogeneous reactions are taken into account by mass source and sink terms in the mass balance equations for solids and gases.

3.2. Solid phase

The solid phase consists of two solid materials at both risers, namely CaO and $CaCO_3$. The total solid phase density is modelled using an empirical correlation to describe the hydrodynamics of the fast fluidised bed. The vertical density profile is modelled using the correlation provided by Johnsson and Leckner [12]

$$\rho_s(h) = \left(\rho_{\mathrm{b}} - \rho_{\mathrm{e}}e^{KH_{\mathrm{e}}}\right)e^{-ah} + \rho_{\mathrm{e}}e^{K(H_{\mathrm{e}}-h)}. \tag{10}$$

Profile decay factors a and K are determined as follows

$$a = 4\frac{u_t}{u_g} \tag{11}$$

$$K = \frac{0.23}{u_g - u_t} \tag{12}$$

where u_t is the particle terminal velocity at the upper part of the riser, u_g is the velocity of gas mixture at the grid and H_e is the height to the exit channel.

The terminal velocity is solved iteratively for the solid particles by giving an initial guess for it and calculating the particle Reynolds number. With the particle Reynolds number the drag coefficient can be solved. The terminal velocity can be calculated from Equation 13 after solving the drag coefficient. This procedure is repeated until a converged solution is found [13].

$$u_t = \left\{\frac{4gd_p}{3C_d}\left(\frac{\rho_s}{\rho_g} - 1\right)\right\}^{0.5} \tag{13}$$

where u_t is terminal velocity of the particles, d_p is the particle diameter, C_d particle drag coefficient, ρ_g the density of the gas phase and ρ_s the apparent density of the solid phase. The solid exit density ρ_{e} has modeled using the following correlation

$$\rho_{\mathrm{e}} = \rho_{s,\mathrm{pt}}\frac{u - u_t}{u_{\mathrm{pt}} - u_t} \tag{14}$$

where u is the gas mixture velocity at the upper part of the riser, u_{pt} is the gas mixture velocity which corresponds pneumatic transport condition, and $\rho_{s,\mathrm{pt}}$ represents the solid density at pneumatic transport condition. The solid bed density ρ_{b} at $h = 0$ is calculated by integrating Eq. (10) over the riser with the riser cross-section area when 0-D solid mass is known. 0-D solid mass balances are solved using the input solid mass flow rate from the other riser and the output solid flows are solved using the empirical correlation

$$\dot{m}_{\mathrm{out}} = kuA_r\rho_{\mathrm{e}}^n \tag{15}$$

where A_r is the cross-section area of the riser. Here parameters k (k<1) and exponent n consider the difference between gas and solid velocity and internal separation of solids flow in the exit region of the reactor.

Time dependent local conversion ratios for element i in the carbonator and calciner can be expressed as

$$\frac{d(m_{s,i}W_{\mathrm{carb},i})}{dt} = \sum_{in} \dot{m}_{s,in}\left(W_{in} - W_i\right) + r_{\mathrm{carb},i} \tag{16}$$

$$\frac{d(m_{s,i}W_{\mathrm{calc},i})}{dt} = \sum_{in} \dot{m}_{s,in}\left(W_{in} - W_i\right) - r_{\mathrm{calc},i} \tag{17}$$

where W_i is the element conversion degree and W_{in} is the conversion degree of the incoming solids.

In the current modelling approach, the riser is divided into the core and wall layer regions. The core-annulus model can be used to simulate the mixing of conversion degree and energy at the risers due to internal recirculation of the solid material observed in fluidised bed reactors. In the core region, the solid material is moving upward and in the wall layer downward. The wall layer flow is transferring solid material from the top of the riser to the bottom region with a conversion degree and energy content corresponding the conditions at the top of the riser. This phenomenon equalizes the conversion degree and temperature level throughout the riser. The thickness and solid density of the wall layer are estimated based on the riser dimensions and fluidising condition. A mass flow entering the wall layer is defined for each element i, based on a given velocity parameter v_{wl}

$$\dot{m}_{\mathrm{s,wl,in}} = v_{\mathrm{wl}}\rho_{s,i}P_i\Delta h_i \tag{18}$$

where P_i and Δh_i are element perimeter and height, respectively. Solids mixing between core and wall layer region is modelled using a back flow ratio k_{bf} which defines the mass flow from the wall layer back to the core region $\dot{m}_{\mathrm{s,wl,out}} = k_{bf}\dot{m}_{\mathrm{s,wl,in}}$.

3.3. Energy balance

In order to solve the time dependent temperatures of the elements, the energy equation of gas-solid suspension is written

$$\frac{dU_i}{dt} = \Delta E_{\mathrm{conv},i} + \Delta E_{\mathrm{disp},i} + \sum_y S_{y,i} - \sum_x Q_{x,i} \tag{19}$$

where ΔE_{conv}, ΔE_{disp}, S_i and Q_i represent convective flows of solids and gas mixture, energy dispersion due to solids mixing, the energy source from chemical reactions and heat transfer rates, respectively. Convective flows are divided into gas and solid phases and treated separately. The following assumptions are made: both phases have the same temperature, the specific heat of solid $c_{p,s}$ is constant, and both phases are incompressible. The convective flows are as follows

$$\begin{aligned} \Delta E_{\mathrm{conv},i} &= \sum_{in} \dot{m}_{in,s,i}c_{p,s}\left(T_{in} - T_i\right) + \frac{dm_{s,i}}{dt}c_{p,s}T_i \\ &+ \sum_{in} \dot{m}_{in,g,i}\left(h_{g,in} - h_{g,i}\right) + \frac{dm_{g,i}}{dt}h_{g,i} \end{aligned} \tag{20}$$

The energy dispersion approach is used to model the transferred energy between the elements due to turbulent motion of the solid material at the riser. Energy dispersion is assumed to follow the form of Fick's law leading energy flux to depend on the vertical temperature gradient.

$$\Delta E_{\mathrm{disp},i} = DA_r^+\bar{\rho}_s^+c_{p,s}\frac{\Delta T^+}{\Delta h_{mp}^+} - DA_r^-\bar{\rho}_s^-c_{p,s}\frac{\Delta T^-}{\Delta h_{mp}^-} \tag{21}$$

where D is the dispersion coefficient for energy mixing and $\bar{\rho}_s$ is the average solids density between elements. The average solid density is calculated between two consecutive elements as an arithmetic average.

Energy sources $S_{y,i}$ from chemical reactions are calculated as follows, using the reaction rate $r_{y,i}$ and reaction enthalpy ΔH_y of the reactions.

$$S_{y,i} = \Delta H_y r_{y,i} \tag{22}$$

For exothermic carbonation reaction ΔH_{carb} = - 1.78 MJ/kg and reverse endothermic calcination reaction ΔH_{calc} = 1.78 MJ/kg.

Heat transfer to the surfaces can be calculated based on the following expression

$$Q_{x,i} = \alpha_{tot} A_{x,i} \left(T_i - T_{x,i} \right), \tag{23}$$

where the total heat transfer coefficient α_{tot} is calculated from the empirical correlation proposed by Dutta-Basu [14]

$$\alpha_{tot} = 5.0 \rho_{s,i}^{0.391} T_i^{0.408}. \tag{24}$$

The final form for the time dependent temperature at element i is

$$\begin{aligned} \frac{dT_i}{dt} m_{s,i} c_{p,s} &= \sum_{in} \dot{m}_{in,s,i} c_{p,s} \left(T_{in} - T_i \right) \\ &+ \sum_{in} \dot{m}_{in,g,i} \left(h_{g,in} - h_{g,i} \right) \\ &+ D A_r^+ \bar{\rho}_s^+ c_{p,s} \frac{\Delta T^+}{\Delta h_{mp}^+} - D A_r^- \bar{\rho}_s^- c_{p,s} \frac{\Delta T^-}{\Delta h_{mp}^-} \\ &+ S_{y,i} - \alpha_{tot} A_{x,i} \left(T_i - T_{x,i} \right) \\ &- \frac{dh_{g,i}}{dt} m_{g,i} \end{aligned} \tag{25}$$

where the last term is calculated using the relation

$$\frac{dh_{g,i}}{dt} m_{g,i} = m_{g,i} \sum_j \frac{dw_{j,i}}{dt} h_j \tag{26}$$

4. Results

In this section, the results from the model are compared against the results from a 30 kW calcium looping test rig of INCAR-CSIC situated in Oviedo, Spain. The rig consists of two circulating fluidised bed reactors with the heights of 6500 mm and diameters of 100 mm. The operating temperatures of the reactors were 650 °C in the carbonator and 700 − 800 °C in the calciner. An accurate description of this test facility and test setup is given by Alonso et al. [15]. Comparison was done by selecting points from the measurements where system operated at steady-state and operational parameters remained nearly constant for a longer period of time. Operational parameters from the experiments where introduced in to the model and system was simulated to a steady-state. The inputs, calculation parameters, and boundary conditions are presented in Figure 2 and Table 1. The parameters not available from the experiments were evaluated based on literature and previous knowledge of the fluidised bed processes. The study of the results concentrates on the carbonator reactor since most of the experimental work has examined its behaviour [8]. With the experimental data available, the study of the capture efficiency and carbonator reactor temperature profile could be done.

Fluidising gas mass flow rate and properties were set based on the experiments and were kept constant during the simulations. Particle diameter and density were assigned from the publication describing the

Table 1: Input parameters of the simulation case

Parameter	
input gas mass flow $\dot{m}_{\mathrm{g,in}}[\mathrm{kg/s}]$	0.0068
input gas temperature $T_{\mathrm{g}}[^{\circ}\mathrm{C}]$	100
input gas CO_2 $w_{\mathrm{CO2,in}}[\mathrm{w}-\%]$	18.1
input gas O_2 $w_{\mathrm{O2,in}}[\mathrm{w}-\%]$	17.2
input gas N_2 $w_{\mathrm{N2,in}}[\mathrm{w}-\%]$	64.7
input gas H_2O $w_{\mathrm{H2O,in}}[\mathrm{w}-\%]$	0.0
solid mass in the reactor $m_{\mathrm{s}}[\mathrm{kg}]$	1.2-2.0
average particle diameter $d_{\mathrm{p}}[\mu\mathrm{m}]$	100
apparent solid density $\rho_{\mathrm{s}}[\mathrm{kg/m^3}]$	1800
number of control volumes $n[-]$	20
kinetic constant $k_{\mathrm{carb}}[\mathrm{m^3kmol^{-1}s^{-1}}]$	25
outside temperature of wall $T_{\mathrm{out}}[^{\circ}\mathrm{C}]$	40
conversion limit of the solid material $W_{\mathrm{max}}[-]$	0.134
calciner temperature $T_{\mathrm{s,in}}[^{\circ}\mathrm{C}]$	800
circulation coefficient $k[-]$	0.4
circulation exponent $n[-]$	0.8
wall layer velocity $v_{\mathrm{wl}}[\mathrm{m/s}]$	0.00005
height of the carbonator [m]	6.5
diameter of the carbonator [m]	0.1

experimental setup [15]. Circulation coefficient k and exponent n were adjusted to match with average solid circulation rate observed in the experiments. Conversion limit of the solid material was set to $W_{\mathrm{max}} = 0.134$ which is a typical value for material undergone several carbonation calcination cycles. Heat losses from the reactor were estimated by setting a thick insulation around the unit and setting a surface temperature for the outside surface. The calciner was not simulated during the carbonator model validation. The conversion degree and temperature of the circulated material coming from the calciner were set as inputs. These values were received from the experiments. Internal circulation and dispersion parameters were selected by comparing the model temperature profile shape to the experimental profile. It was confirmed that the modelled temperature profile agrees with experimental one, when the dispersion coefficient and wall layer flow are very low and consequently the backflow from the wall layer was also set zero. Because of the high aspect ratio of the experimental unit, it is reasonable to assume that the lateral effects are minimal. The validity of the reaction rate model was tested by comparing the capture efficiency as a function of solid inventory between simulations and experiments for the given inputs, Figure 3.

As expected, the capture efficiency increases steadily when inventory is added and the simulated capture efficiencies showed excellent agreement with the experiments. Although the capture efficiencies are well predicted, the temperature of the lower bed is over predicted in the simulations when inventory increases, Figure 4. This discrepancy is mainly caused by the fact that the cooling of the experimental carbonator was done in practise by removing the insulation, when the temperature of the reactor increased. These changes were not included in the model calculations. The lower bed temperature has a considerable effect on the carbonator performance because the majority of the active material is situated there. If the temperature rises over the equilibrium condition, a sharp decrease in the capture efficiency will be experienced. This will eventually happen if inventory is added and no cooling is introduced to the reactor. In larger scales, evaporator surfaces or internal heat exchangers will be necessary to control the carbonator temperature in the desired region. In Figures 5 and 6 the vertical temperature profile of the carbonator is presented with two different inventories. The lower inventory profile agrees well with the temperature measurements from the experimental rig. With the higher inventory, the simulated temperature profile moves away from the ideal region, but preserves the similar shape as in the experiment. In the experiments, the insulation was removed,

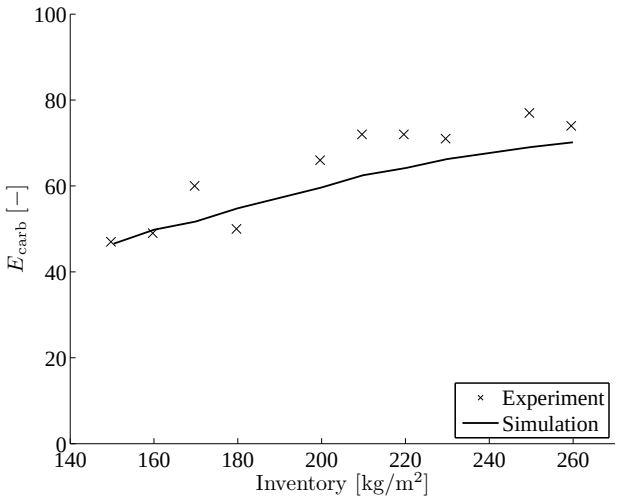

Figure 3: Capture efficiency from the experiments compared to the model capture efficiency as a function of solid inventory

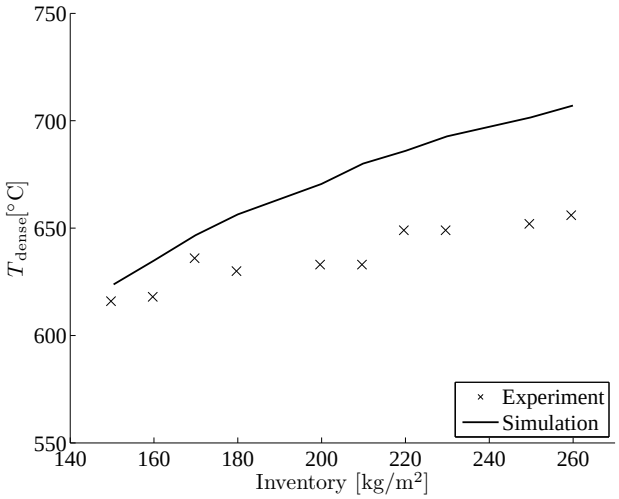

Figure 4: Model lower bed temperature compared with the experimental results as a function of solid inventory

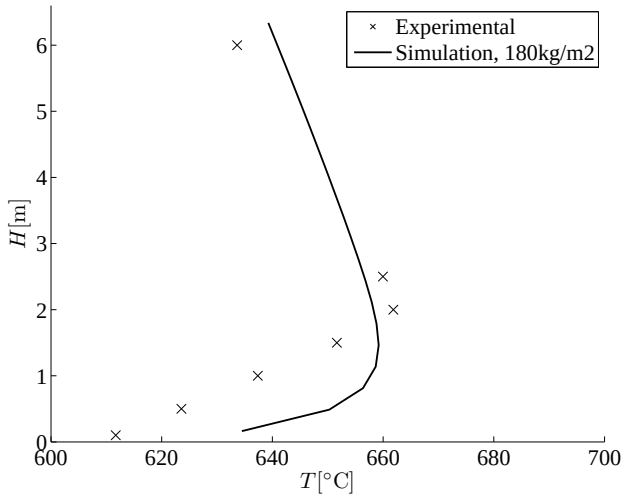

Figure 5: Vertical temperature profile for the model and test rig carbonator with 180 kg/m^2 solid inventory

which lowered the temperature. Better agreement could have been seen, if the insulation thickness in the model would have been changed accordingly. In the model, the details of changes in insulation materials were not considered in the thermal boundary conditions and that is why the simulated temperature curve is higher than the measured. In Figure 7, the vertical conversion profile is presented for the 180 kg/m^2 inventory simulation. In the dense lower region, conversion degree reaches quickly the theoretical limit defined by the active solids in the system. In the model, the mixing of solids through the wall layer has a strong effect on the conversion degree profile, evening out the conversion degree difference between reactor entrance and exit. With no experimental information of the conversion degree, the intensity of the solid mixing had to be determined from incoming and leaving solid conversion degrees with the help of pressure, and temperature profiles. Ultimately, the construction and fluidisation mode of the reactor will determine how the core-annulus flow is formed. In larger units, where the aspect ratio allows more solid movement in the horizontal direction, the role of the phenomenon needs to be studied.

5. Conclusion

A 1-dimensional dynamical model for the calcium looping process utilizing two interconnected fluidised bed reactors was developed. The model was tested against a laboratory scale (100 mm x 6500 mm) test rig at INCAR-CSIC. First results show good agreement between the experimental observations and simulations. The simulated and experimental capture efficiencies agree well, if the temperature boundary conditions are well described. Sensitivity of the results to the reactor temperature modelling, confirms the necessity of the detailed description of energy conservation equation within the reactor. This feature is absent in most previously introduced models. Furthermore, the process simulations conducted with full calcium looping cycle confirmed the need for temperature control for the efficient operation of this system. Especially the significance of cooling in the carbonator was clearly seen, when the carbonator reactivity increased. In the studied system with large aspect ratio, the flow is essentially 1-D and 3-D effects may be neglected. However, in larger units the effect of wall layer recirculation and energy distribution by dispersion may be significant and needs to be verified. In studied system of interconnected fluidised beds with several parallel reactions, the process operation is affected by many different parameters, such as recirculation ratio, fluidisation conditions, cooling and heating, fuel feed, make-up flow and solid inventory. The capability to model properly the hydrodynamics, reaction kinetics, and energy transfer of this complex system is an important step towards scaling up and commercialization of this promising carbon capture and storage technology.

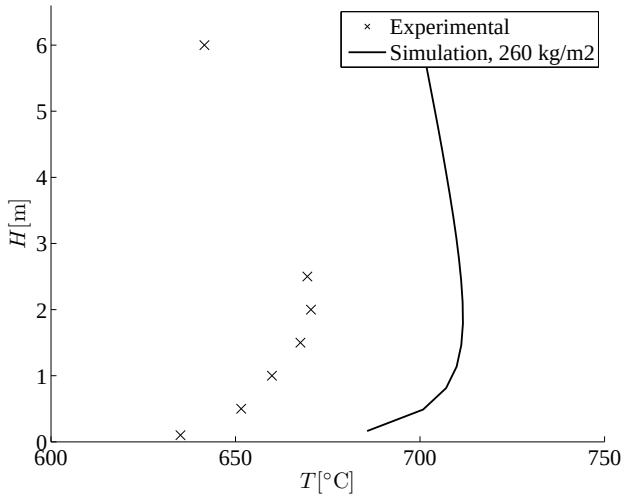

Figure 6: Vertical temperature profile for the model and test rig carbonator with 260 kg/m^2 solid inventory

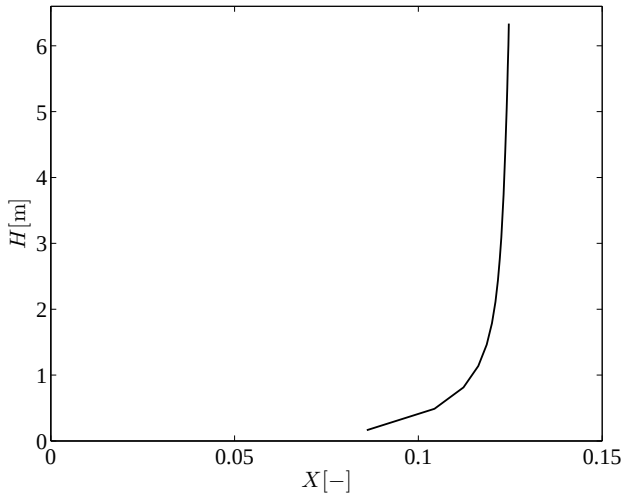

Figure 7: Vertical conversion profile for the model

6. Acknowledgements

This work has been done in participation to the EU Framework Programme 7 CaOling project.

7. References

[1] T. Shimizu, T. Hirama, H. Hosoda, K. Kitano, M. Inagaki, K. Tejima, A twin fluid-bed reactor for removal of CO2 from combustion processes, Chemical Engineering Research and Design 77 (1) (1999) 62 – 68.

[2] G. Grasa, J. Abanades, Narrow fluidised beds arranged to exchange heat between a combustion chamber and a CO2 sorbent regenerator, Chemical Engineering Science 62 (1-2) (2007) 619 – 626, Fluidized Bed Applications.

[3] M. Alonso, N. Rodríguez, G. Grasa, J. Abanades, Modelling of a fluidized bed carbonator reactor to capture CO2 from a combustion flue gas, Chemical Engineering Science 64 (5) (2009) 883 – 891.

[4] N. Rodriguez, M. Alonso, J. C. Abanades, A. Charitos, C. Hawthorne, G. Scheffknecht, D. Y. Lu, E. J. Anthony, Comparison of experimental results from three dual fluidized bed test facilities capturing CO2 with CaO, Energy Procedia 4 (0) (2011) 393 – 401, 10th International Conference on Greenhouse Gas Control Technologies.

[5] C. Hawthorne, M. Trossmann, P. G. Cifre, A. Schuster, G. Scheffknecht, Simulation of the carbonate looping power cycle, Energy Procedia 1 (1) (2009) 1387 – 1394, Greenhouse Gas Control Technologies 9, Proceedings of the 9th International Conference on Greenhouse Gas Control Technologies (GHGT-9), 16-20 November 2008, Washington DC, USA.

[6] A. Lasheras, J. Ströhle, A. Galloy, B. Epple, Carbonate looping process simulation using a 1D fluidized bed model for the carbonator, International Journal of Greenhouse Gas Control 5 (2011) 686–693.

[7] A. Charitos, N. Rodriguez, C. Hawthorne, M. Alonso, M. Zieba, B. Arias, G. Kopanakis, G. Scheffknecht, J. C. Abanades, Experimental validation of the calcium looping CO2 capture process with two circulating fluidized bed carbonator reactors, Industrial & Engineering Chemistry Research 50 (16) (2011) 9685–9695.

[8] N. Rodriguez, M. Alonso, J. C. Abanades, Experimental investigation of a circulating fluidized-bed reactor to capture CO2 with CaO, AIChE Journal 57 (5) (2011) 1356–1366.

[9] D. Alvarez, J. C. Abanades, Determination of the critical product layer thickness in the reaction of CaO with CO2, Industrial & Engineering Chemistry Research 44 (15) (2005) 5608–5615.

[10] G. S. Grasa, J. C. Abanades, CO2 capture capacity of CaO in long series of carbonation/calcination cycles, Industrial & Engineering Chemistry Research 45 (26) (2006) 8846–8851.

[11] F. García-Labiano, A. Abad, L. F. de Diego, P. Gayán, J. Adánez, Calcination of calcium-based sorbents at pressure in a broad range of CO2 concentrations, Chemical Engineering Science 57 (13) (2002) 2381 – 2393.

[12] F. Johnsson, B. Leckner, Vertical distribution of solids in a CFB-furnace, in: K. Heinschel (Ed.), Proceedings of the 13th International Conference on Fluidized Bed combustion, 1995, pp. 671–679, Orlando, FL, USA. May 07-10.

[13] D. Kunii, O. Levenspiel, Fluidization Engineering, 2nd Edition, Butterworth-Heinemann, 1991.

[14] A. Dutta, P. Basu, Overall heat transfer to water walls and wing walls of commercial circulating fluidized bed boilers, J. Inst. Energy 75 (2002) 85–90.

[15] M. Alonso, N. Rodríguez, B. González, G. Grasa, R. Murillo, J. Abanades, Carbon dioxide capture from combustion flue gases with a calcium oxide chemical loop. experimental results and process development, International Journal of Greenhouse Gas Control 4 (2) (2010) 167 – 173, The Ninth International Conference on Greenhouse Gas Control Technologies.